

## ARTICLE

# Interaction between LIS1 and doublecortin, two lissencephaly gene products

Michal Caspi, Roe Atlas, Ayelet Kantor, Tamar Sapir and Orly Reiner\*

Department of Molecular Genetics, Weizmann Institute of Science, 76100 Rehovot, Israel

Received 7 June 2000; Revised and Accepted 24 July 2000

**Mutations in either LIS1 or DCX are the most common cause for type I lissencephaly. Here we report that LIS1 and DCX interact physically both *in vitro* and *in vivo*. Epitope-tagged DCX transiently expressed in COS cells can be co-immunoprecipitated with endogenous LIS1. Furthermore, endogenous DCX could be co-immunoprecipitated with endogenous LIS1 in embryonic brain extracts, demonstrating an *in vivo* association. The two protein products also co-localize in transfected cells and in primary neuronal cells. In addition, we demonstrate homodimerization of DCX *in vitro*. Using fragments of both LIS1 and DCX, the domains of interaction were mapped. LIS1 and DCX interact with tubulin and microtubules. Our results suggest that addition of DCX and LIS1 to tubulin enhances polymerization in an additive fashion. In *in vitro* competition assays, when LIS1 is added first, DCX competes with LIS1 in its binding to microtubules, but when DCX is added prior to the addition of LIS1 it enhances the binding of LIS1 to microtubules. We conclude that LIS1 and DCX cross-talk is important to microtubule function in the developing cerebral cortex.**

## INTRODUCTION

Development of the human brain is a complex process, which initiates in the prenatal stage and is completed in the first years of childhood. Corticogenesis involves processes such as proliferation, migration and differentiation that leads to the formation of the mature convoluted cortex. Defects in neuronal migration may result in lissencephaly that is a severe brain malformation characterized by the lack of most gyri and sulci. There are two types of lissencephaly: type I or 'classical lissencephaly', where four layers of abnormally positioned neurons are observed in the neocortex, and type II or 'cobblestone' lissencephaly, where the cortex is unlayered (1). Mutations in two different genes may result in type I lissencephaly: *LIS1*, an autosomal gene located on chromosome 17p13.3 (2), and *doublecortin*, an X-linked gene (3,4). The phenotypic presentation of the patients is very similar, with delayed development and magnetic resonance imaging (MRI) analysis revealing both agyria and pachygyria. However, whereas the frontal brain is more affected in patients with mutations in *doublecortin*, the parietal and occipital cortex are more affected in the case of mutations in *LIS1* (5). Mutations in the X-linked *DCX* gene result in lissencephaly in males or subcortical laminar heterotopia, i.e. 'double cortex', in females (3,4). The milder phenotype seen in females consists of a brain with bilateral plates or bands of gray matter located beneath the cortex and ventricle but separated from both, hence the descriptive term double cortex (6). Mutations in *LIS1* are hemizygous and the disease results from reduced gene dosage (2). The primary amino acid sequence reveals that LIS1 contains seven WD (tryptophan–aspartic acid) repeats (2,7,8), positioning LIS1 in

a large group of proteins known to be involved in multiple protein interactions (9). Although LIS1 was isolated as a subunit of platelet-activating factor acetylhydrolase Ib (10), the protein also interacts with microtubules and affects microtubule dynamics (11). The product of the *doublecortin* gene associates with and stabilizes microtubules (12–14). We have identified the tubulin-binding domain of DCX and found it to be an evolutionarily conserved repeat (15). Interestingly, most lissencephaly-causing amino acid substitutions in DCX cluster within the repeated domain (15). Our combined results emphasize the importance of LIS1–microtubule and DCX–microtubule interactions during normal and abnormal brain development. As LIS1 and DCX have similar functions, we raised the hypothesis that they may interact directly. Our results suggest that LIS1 and DCX are co-expressed, interact and can function in the same protein complex in the developing brain.

## RESULTS

### Co-expression and co-localization of LIS1 and DCX

To follow expression of LIS1 and DCX during brain development we examined RNA expression in the dorsal telencephalon of mouse embryos beginning at embryonic day E10.5–E15.5, when the process of neurogenesis is active. Although LIS1 is clearly expressed at all time points examined, the expression of DCX initiates at E11.5 and increases later on (Fig. 1). This result reflects the notion that both genes are expressed in the developing brain as has been shown (13,16). Next, we examined whether the two protein products are co-expressed in the same

\*To whom correspondence should be addressed. Tel: +972 8 9342319; Fax: +972 8 9344108; Email: orly.reiner@weizmann.ac.il

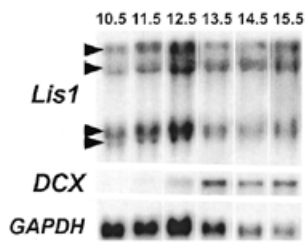


**Figure 1.** Expression of Lis1 and DCX RNA in the dorsal telencephalon. Total RNA (7.5 µg) from the dorsal telencephalon of several mouse embryos from different embryonic days (E10.5–E15.5) was loaded onto an agarose gel and northern blotted. The blot was probed with Lis1, DCX and GAPDH probes as indicated. The four Lis1 mRNA species are indicated by arrowheads. DCX expression is visible at E11.5. Loading was assessed by hybridization with GAPDH.

neurons. As can be seen (Fig. 2), the staining in neurons suggested co-localization of both proteins. However, the co-localization in the neurons is partial: quite strikingly, LIS1 antibodies react with thin neurites that DCX antibodies do not recognize. Both antibodies stain the soma and the thick neurites. Nevertheless, DCX immunostaining is lacking from at least one of the neurites that may be the future axon, suggesting polarity in DCX neuronal localization. In order to further investigate the co-localization, we transiently transfected COS-7 cells that endogenously express LIS1 with FLAG-tagged DCX and immunostained them. The transfected cells depict a significant overlap in the staining pattern (Fig. 3). The DCX-transfected cells exhibit a marked change in their morphology in comparison with untransfected cells, caused by the bundled microtubules. This co-localization prompted us to investigate further potential interactions between LIS1 and DCX.

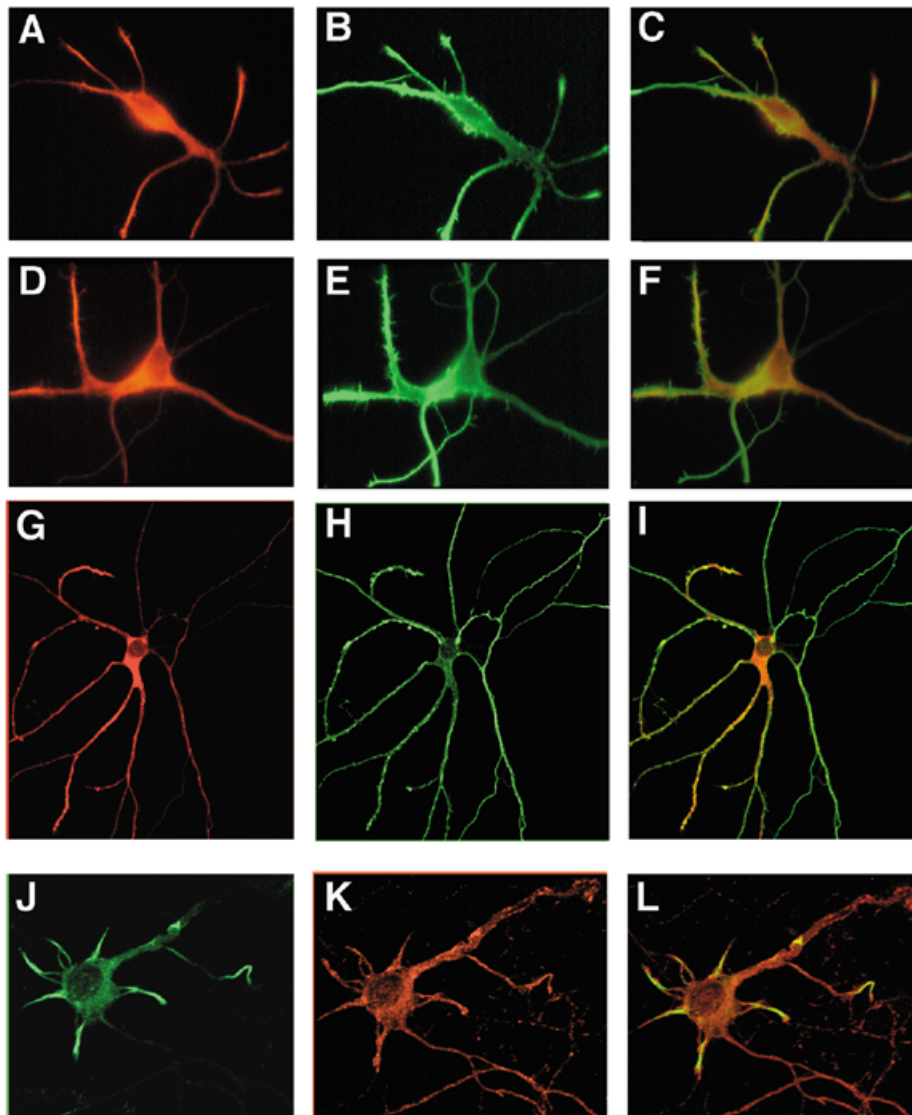


**Figure 2.** Cellular localization of DCX and LIS1 proteins in neurons. Rat hippocampal primary neurons were co-stained with rabbit anti-LIS1 (affinity purified) and mouse anti-DCX antibodies. (A, D and G) Primary mouse anti-DCX antibodies and secondary anti-mouse–rhodamine. (B, E and H) Primary rabbit anti-LIS1 and secondary anti-rabbit–FITC. (J) Primary mouse anti-DCX and secondary anti-mouse–FITC. (K) Primary rabbit anti-LIS1 and secondary anti-rabbit–rhodamine. (C, F, I and L) Computer-derived overlay. (A–F) Olympus microscope; 100× magnification; (G–L) confocal microscope; 40× magnification.

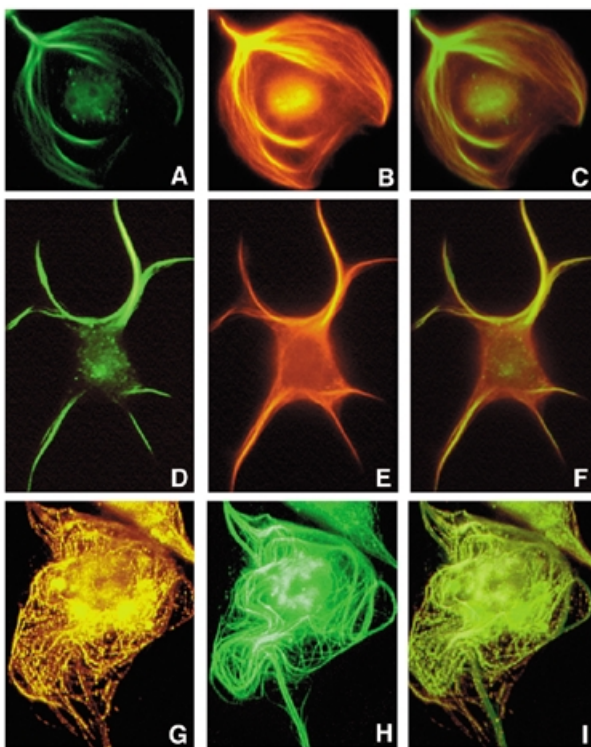


**Figure 3.** Cellular localization of DCX and LIS1 in COS-7 cells. COS-7 cells were transfected with FLAG-DCX and fixed after 48 h. Co-staining was performed with either anti-LIS1 and anti-FLAG antibodies or anti-LIS1 and anti-DCX. (A and D) Primary rabbit anti-LIS1 and secondary anti-rabbit-FITC. (B and E) Primary mouse anti-FLAG and secondary anti-mouse-rhodamine. (G) Primary rabbit anti-LIS1 and secondary anti-rabbit-rhodamine. (H) Primary mouse anti-DCX and secondary anti-mouse-FITC. (C, F and I) Overlap of co-staining.

### LIS1 and DCX interact *in vitro*

Several assays performed with recombinant proteins demonstrated a possible interaction between LIS1 and DCX. We used BIAcore, a system that measures changes in surface plasmon resonance that are proportional to the changes in the mass of molecular species bound to the surface (17–20). The mass differences measured reflect the kinetic events including association and dissociation of complexes that are composed of immobilized molecules and other molecules brought into contact with them in the flow cell. Binding of DCX to immobilized LIS1 is specific and dose dependent as it is proportional to the amount of bound LIS1 protein (ligand levels) (Fig. 4). This was the first indication that LIS1 and DCX can interact directly without additional mediators.

### Mapping of interaction domains

**LIS1-DCX heterodimerization and DCX homodimerization.** To map the region within DCX that interacts with LIS1, we used several glutathione *S*-transferase (GST)-DCX fragments (schematic presentation shown in Fig. 5A): full-length DCX (amino acids 1–360), amino acids 110–360, amino acids 1–213 (12), pep1 (amino acids 51–135), pep2 (amino acids 178–259), and pep(1+2) (amino acids 51–259) (15). Full-length GST-DCX pulled down recombinant LIS1 (Fig. 5B), as well as *in vitro*

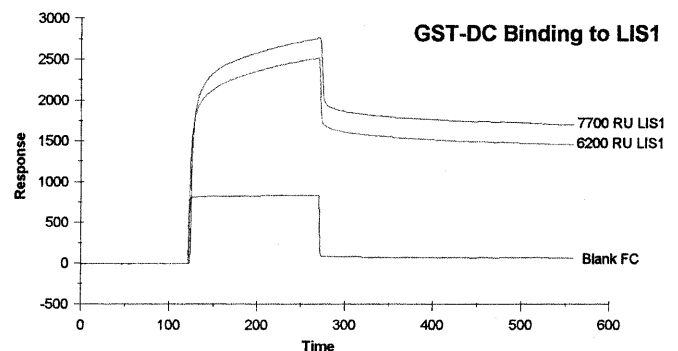


**Figure 4.** LIS1-DCX interaction using surface plasmon resonance. LIS1 was immobilized to the sensor chip at two densities [7700 and 6200 resonance units (RU)]. The time is in minutes. A blank channel was prepared by a flow buffer instead of protein solution during the immobilization phase. GST-DCX (5 mM) was introduced to the immobilized LIS1 at a constant flow rate of 10 ml/min. As can be seen in the two channels GST-DCX is bound by the LIS1 protein in a dose-specific manner.

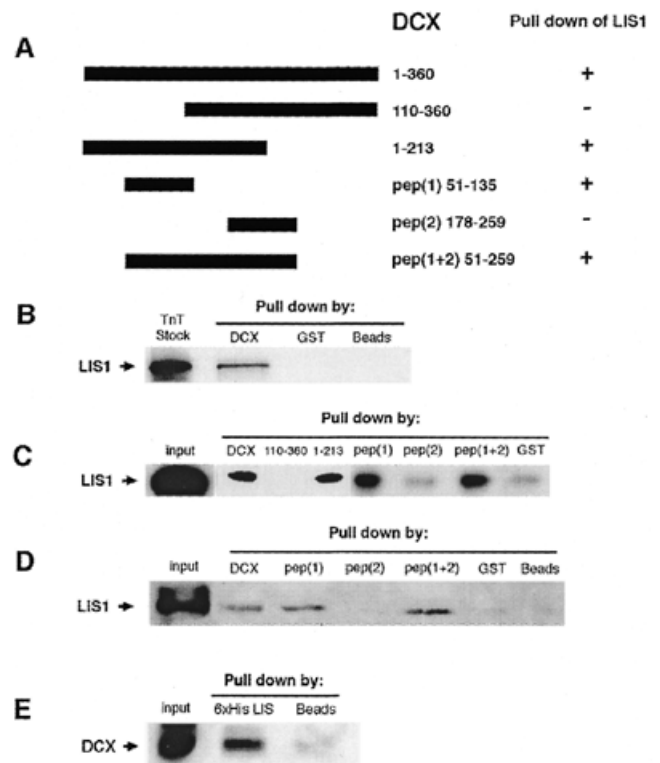


**Figure 5.** Interaction of DCX and LIS1 *in vitro* using pull-down assays. (A) Schematic presentation of the different recombinant GST-DCX fragments used in the experiment. (B) 6xHis-LIS1 translated in a rabbit reticulocyte system labeled with [<sup>35</sup>S]methionine and pulled-down by GST-DCX and GST control. (C) 6xHis-LIS1 expressed and purified from insect cells was pulled down by GST fusion full-length and shorter fragments of DCX. (D) LIS1 was also pulled down from embryonic brain extract. (E) Reciprocally, DCX from embryonic brain extract was pulled down by 6xHis-LIS1. Localization of the interaction site was done by using GST-pep(1), -pep(2) and -pep(1+2) of DCX (C and D). From both panels it is clear that the minimal fragment required for this *in vitro* interaction is pep(1) (amino acids 51–135) of DCX.

translated LIS1 (Fig. 5C) and endogenous LIS1 from embryonic brain extract (Fig. 5D). The smallest portion of DCX that pulls

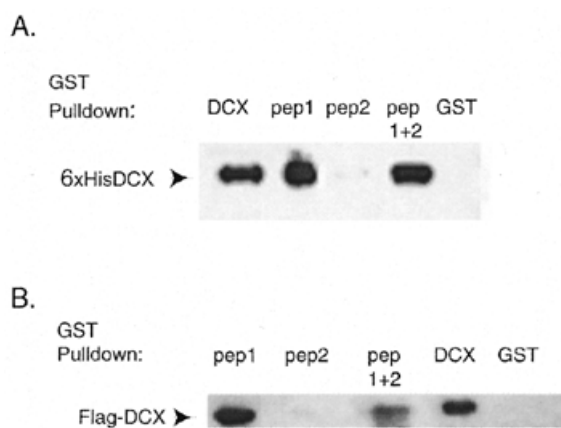


**Figure 6.** *In vitro* DCX homodimerization. (A) 6xHis-DCX expressed and purified from bacterial cells was pulled down by GST fusion full-length and shorter fragments of DCX (pep1, pep2 and pep1+2). GST was used as a negative control. (B) FLAG-tagged DCX was transfected to 293T cells and pulled down by GST fusion full-length and shorter fragments of DCX (pep1, pep2 and pep1+2). GST was used as a negative control. From both panels it is clear that the minimal fragment required for this *in vitro* interaction is pep(1) (amino acids 51–135) of DCX.

down LIS1 is pep1. Our previous results (15) identified this region as an evolutionarily conserved domain. This peptide was also shown to pull down tubulin from brain extract, but did not pull down purified tubulin (15). The peptide probably recruited additional proteins from the extract that mediated its interaction with tubulin. It may be that LIS1 mediates pep1–tubulin interaction.

In addition, we detected *in vitro* homodimerization of DCX. This was demonstrated by pull-down of recombinant DCX tagged with 6xHis or GST (Fig. 6A), and in COS cell extracts where FLAG–DCX was pulled down by GST–DCX (Fig. 6B). The homodimerization domain was mapped to the pep1 domain of DCX as described previously (Fig. 6). Our finding of a common interaction region responsible for DCX homodimerization and LIS1–DCX interaction predicted that LIS1 and DCX compete.

In a similar fashion, we mapped the reciprocal regions in LIS1 that are important for DCX binding. Previous studies with LIS1 have indicated that simple truncations result in a protein that is not folded properly (21). However, our recent work suggests that LIS1 is a  $\beta$ -propeller similar to the  $\beta$ -subunit of G proteins (21,22) and therefore it is likely that each WD will retain its structure as an anti-parallel  $\beta$  sheet. Based on this assumption, we cloned individual WD domains of LIS1 and the N-terminal portion (schematic presentation shown in Fig. 7A), translated them *in vitro* and used GST–DCX in a pull-down experiment. The results were plotted as the percentage of input protein that was pulled down by GST–DCX. According to this type of analysis the main WD repeat that participates in the LIS1–DCX interaction is WD7.

**LIS1 and DCX interact *in vivo*.** To examine LIS1–DCX interaction *in vivo*, 293T cells were transiently transfected with PECE–FLAG–DCX constructs. The constructs harbor normal DCX or mutations that were identified in patients (T203R, R192W, Y125H, D62N, R59L and S47R) (3,4,15). Immunoprecipitation

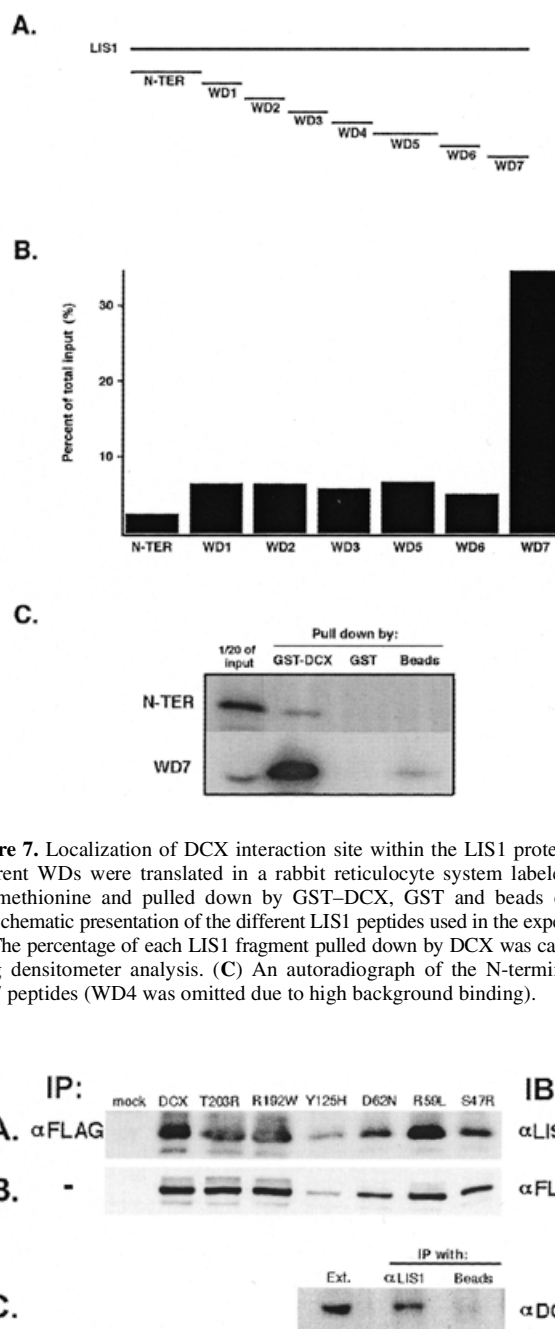


**Figure 7.** Localization of DCX interaction site within the LIS1 protein. The different WDs were translated in a rabbit reticulocyte system labeled with [<sup>35</sup>S]methionine and pulled down by GST–DCX, GST and beads control. (A) Schematic presentation of the different LIS1 peptides used in the experiment. (B) The percentage of each LIS1 fragment pulled down by DCX was calculated using densitometer analysis. (C) An autoradiograph of the N-terminal and WD7 peptides (WD4 was omitted due to high background binding).

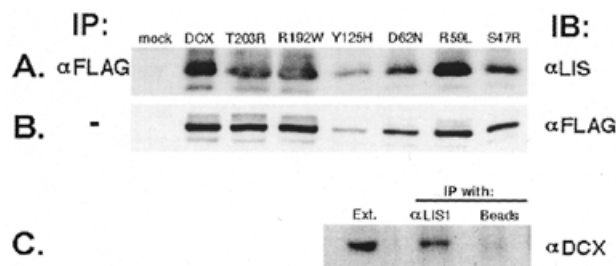


**Figure 8.** Interaction of DCX and LIS1 *in vivo*. (A) 293T cells were transfected with normal and mutated FLAG–DCX constructs. Immunoprecipitation assay was performed after 48 h using anti-FLAG agarose beads. The reactions were immunoblotted and detection was done using monoclonal anti-LIS1 antibodies (clone 210). All the different mutant, as well as the normal, DCX proteins interact with endogenous LIS1. (B) The level of expression of the different FLAG–DCX constructs by western blot of the extract using anti-FLAG antibodies. (C) Immunoprecipitation of DCX from embryonic brain extract was performed with anti-LIS1 monoclonal antibodies (clone 338). A western blot analysis detected the presence of DCX in the immunoprecipitated material using rabbit anti-DCX antibodies.

using anti-FLAG antibodies successfully precipitated endogenous LIS1 from transfected cells, but not from mock-transfected cells (Fig. 8A). DCX mutations were expressed, as

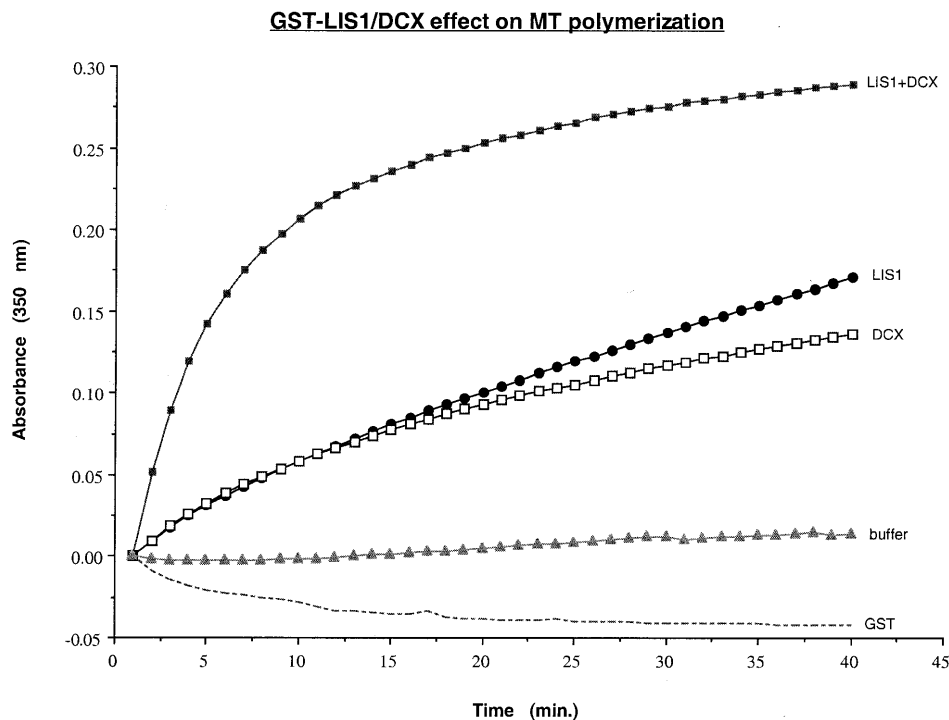


**Figure 9.** DCX and LIS1 affect tubulin assembly rate *in vitro*. The assembly rate of tubulin was measured using a light scattering assay. The concentration of tubulin used was 15 mM. The optical absorbance was recorded every minute for 40 min. The recombinant proteins used were GST, GST-DCX and GST-LIS1, each at a final concentration of 7.5 mM. The recombinant proteins were added prior to the measurement. Addition of the two proteins together (each at a concentration of 7.5 mM) shows that they have an additive effect on tubulin polymerization.

demonstrated by western blot using anti-FLAG antibodies (Fig. 8B).

Next we wanted to test whether LIS1-DCX interactions occurred in the developing mouse brain. LIS1 from embryonic brain extracts was immunoprecipitated using mouse monoclonal anti-LIS1 antibodies, protein A/G beads or anti-GAD antibodies (data not shown). Co-immunoprecipitation with DCX was checked by immunoblotting with anti-DCX antibodies (Fig. 8C). A DCX-immunoreactive band was detected specifically in the anti-LIS1 precipitate but not in the control precipitates. These studies suggest that LIS1 and DCX form a complex in the developing brain.

*LIS1, DCX and tubulin.* To explore whether LIS1 and DCX affect microtubule formation in an additive or competitive way, we measured the assembly rate of tubulin using a light scattering assay (Fig. 9). This assay is based on the increase in optical scattering as microtubules polymerize, measured as an effective optical density. Addition of DCX to tubulin increased the assembly rate of tubulin as shown previously (12). Addition of LIS1 to tubulin without DCX also increased the polymerization rate of microtubules (Fig. 9). When LIS1 was added to tubulin in the presence of DCX the assembly rate of tubulin increased in an additive fashion (Fig. 9). If LIS1 and DCX share the same tubulin binding sites we would expect the net result not to be additive since the proteins compete for the same interaction region. The results of this experiment suggest that LIS1 and DCX bind to different sites on tubulin or that they share common sites. If the latter possibility is correct and they share

common sites, the additive effect may be explained by altered binding affinities.

To differentiate between these two possibilities we designed a competition assay where both proteins were added to pre-assembled microtubules. In the first experiment, increasing amounts of DCX were added to constant amounts of LIS1 (Fig. 10A); whereas in the second experiment, increasing amounts of LIS1 were added to constant amounts of DCX (Fig. 10B). The distribution of LIS1 between the insoluble (pellet) microtubule fraction and the soluble (supernatant) fraction was examined by western blot analysis. Interestingly, the results changed depending on the order in which the components were added. When increasing amounts of DCX were added to constant amounts of LIS1, DCX competes LIS1 out and more LIS1 was found in the supernatant fraction (Fig. 10A). When increasing amounts of LIS1 were added to constant amounts of DCX, the affinity of LIS1 to microtubules increased and more LIS1 was found in the pellet fraction (Fig. 10B). Addition of LIS1 did not change the affinity of DCX to the microtubule cytoskeleton (data not shown), and DCX was found mainly in the pellet fraction. In these experiments the net amount of polymerized microtubules did not change (Fig. 10C).

## DISCUSSION

To investigate molecular mechanisms involved in lissencephaly, we tested for an interaction between LIS1 and DCX using several independent methods. The notion that two genes,

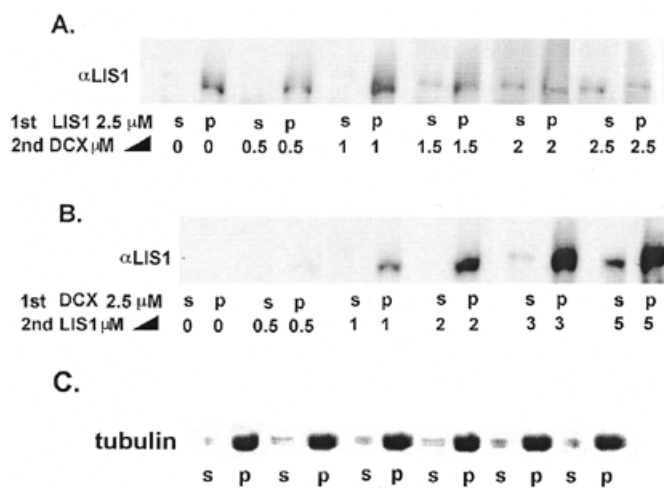


**Figure 10.** LIS1, DCX and tubulin competition assays. The relative distribution of LIS1 in the soluble fraction (s) and microtubule-associated pellet (p) was determined by western blot analysis using anti-LIS1 monoclonal antibodies. (A) Constant concentration of LIS1 (2.5  $\mu$ M) was added to pre-assembled microtubules, then increasing concentrations of DCX was added to the mixture. Note that with the addition of 1.5  $\mu$ M DCX, LIS1 shifts to the soluble fraction. (B) Constant concentration of DCX (2.5  $\mu$ M) was added to pre-assembled microtubules, then increasing concentrations of LIS1 were added to the mixture. Pre-incubating the pre-assembled microtubules with DCX result in the presence of more LIS1 in the pellet fraction [for example, compare 2  $\mu$ M DCX and 2.5  $\mu$ M LIS1 in (A) with 2  $\mu$ M LIS1 and 2.5  $\mu$ M DCX in (B)]. (C) A representative gel showing microtubule polymerization. The gels were stained with Coomassie brilliant blue and the relative amounts of tubulin in the pellet and supernatant are shown.

which when mutated give rise to a similar phenotype, can physically interact has been demonstrated in the past. Two gene products involved in autosomal dominant polycystic disease, PKD1 and PKD2, interact via similar coiled-coil domains in the C-terminal region (23,24). Naturally occurring pathogenic mutations in PKD1 and PKD2 disrupt their associations (23). An additional example are two genes involved in tuberous sclerosis (TSC) an autosomal dominant disorder characterized by a broad phenotypic spectrum that includes seizures, mental retardation, renal dysfunction and dermatological abnormalities. Mutations in the *TSC1* and *TSC2* genes were found to be responsible for the disease. The two gene products can interact with each other (25,26). Careful investigations suggested the presence of additional proteins within this complex (27). It has been proposed that one of these proteins modifies the self-aggregation of the other.

We have shown that LIS1 and DCX are co-expressed in the developing brain. Furthermore, the two proteins co-localize in transfected COS cells and partially co-localize in primary neurons. In neuronal cells it was observed that DCX localization is polar. We plan to investigate this issue more carefully in the future, as polarized morphology of neurons, typified by a single long axon and several short dendrites is a fundamental morphological feature (28). LIS1 immunostaining, on the other hand, was obvious in very fine dendrites. This may be related to the recent observation that heterotopic pyramidal neurons in *Lis1*<sup>-/-</sup> mice were stunted and possessed fewer dendritic branches (29).

The actual interaction of the two gene products was demonstrated as the recombinant proteins interacted in the BIAcore and pull-down assays. Mapping of the interaction domains was feasible using pull-down assays with short peptides of either LIS1 or DCX. The minimal interacting regions are the last WD repeat in LIS1 (WD7) and pep1 in DCX. In addition to DCX heterodimerization, we also showed that DCX is capable of homodimerization *in vitro*. The interaction domains of DCX with both DCX or LIS1 were mapped to an evolutionarily conserved region (pep1, amino acids 52–133) (15), which includes the tubulin binding site as well. The existence of such a complex *in vitro* suggests that it may also function *in vivo*. Indeed, the LIS1–DCX interaction *in vivo* was demonstrated by co-immunoprecipitation of transiently expressed DCX in transfected cells with endogenous LIS1. Moreover, the two proteins were co-immunoprecipitated in embryonic brain extracts that express both LIS1 and DCX. In transfected cells, we tested the interaction of six naturally occurring pathogenic mutations of DCX with LIS1. Some of the mutations were not expected to alter interactions because they are located outside the interaction domain mapped using the pull-down experiments. However, point mutations may affect protein folding; therefore, we thought that it may be useful to test all the mutated proteins we had. The mutations that we tested did not interfere with the association between LIS1 and DCX.

We have previously demonstrated that both LIS1 and DCX interact with tubulin therefore, we cannot exclude the possibility that *in vivo* interactions between DCX and LIS1 are mediated by tubulin. Thus, we tested the effect of both proteins on microtubule polymerization. Using a light scattering assay it was observed that the addition of both proteins result in an additive effect on microtubule polymerization. This suggested two possibilities: (i) LIS1 and DCX have different binding sites thus their binding is additive; or (ii) these proteins share regions but perhaps the interaction of one with tubulin changes the binding affinity of the other. In order to distinguish between these possibilities we designed a competition assay where increasing concentrations of DCX were added to constant concentrations of LIS1 with pre-assembled microtubules or vice versa. Interestingly, the results were dependent on the order of the added components (a schematic model is shown in Fig. 11). In this set of experiments LIS1 was usually found associated with the microtubule pellet fraction (Fig. 11A); however, when DCX was added it competed with LIS1 and more was found in the soluble fraction (Fig. 11B). DCX, on the other hand was completely associated with microtubules regardless of LIS1 concentration (Fig. 11C and D). When LIS1 was added to the microtubule–DCX complex a larger amount of LIS1 was then associated with the microtubule pellet fraction (Fig. 11D). This alteration in the binding affinity of LIS1 may be due to a conformational change in the microtubules themselves (Fig. 11C and D). Can this experiment reflect *in vivo* behaviour of these molecules? Can the presence of one molecule affect the function of the other? Although this indeed is far fetched, there may be some evidence to support this hypothesis. In COS cells transfected with DCX, we noticed a shift of endogenous LIS1 (usually partially associated with microtubules) to be more associated with microtubules. This question will be addressed more directly in the future using DCX transgenic mice.

Is LIS1–DCX interaction relevant to the lissencephaly phenotype? We believe that it is. A recent study (30) of

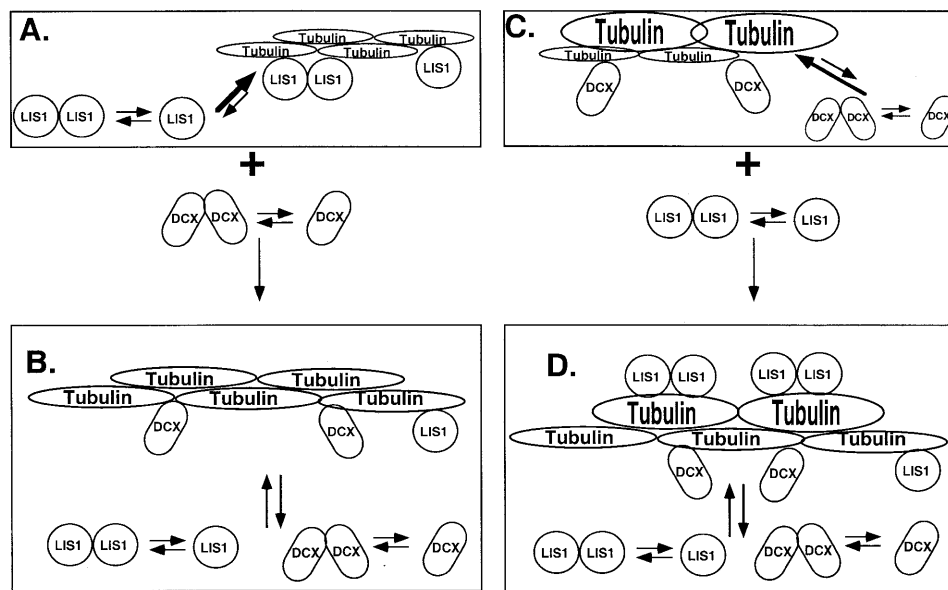


**Figure 11.** A schematic model for the LIS1–DCX–microtubule interaction. (A) When LIS1 was added to pre-assembled microtubules most of the LIS1 molecules (dimers or monomers) interacted with microtubules. (B) DCX competes with LIS1 and less LIS1 is found in the microtubule-associated fraction. (C) When DCX was added to pre-assembled microtubules most of the DCX molecules interacted with microtubules. (D) On the other hand, increasing concentrations of LIS1 added to the DCX–microtubule complexes caused LIS1 to bind microtubules with a higher affinity (plausibly due to a conformational change that may be in the microtubule moiety). As a result, more of LIS1 is bound to microtubule.

immunohistochemical expression of DCX demonstrated abnormal localization in Miller–Dieker syndrome (involving LIS1 deletion) and Fukuyama congenital muscular dystrophy but not in other migration disorders. This result taken together with our findings provides further evidence for a possible endogenous function for LIS1–DCX–tubulin complex.

## MATERIALS AND METHODS

### Northern blot

Total mRNA for northern analysis was isolated using Tri Reagent (Sigma, Rehovot, Israel) according to the manufacturer's protocol. Northern blots were performed as described by Ausubel *et al.* (31).

### Cell culture

COS-7 and 293T cells were grown at 37°C with 5% CO<sub>2</sub> and 95% air in DMEM nutrient medium supplemented with 10% fetal bovine serum, 4 mM glutamine, 100 U/ml penicillin and 0.1 mg/ml streptomycin. Cultures were split using standard trypsinization procedures. Cells were transfected using the BES transfection procedure (31). Transfected cells were harvested or stained after 48 h. Efficiency of transfections was estimated using an EGFP expression vector (Clontech, Palo Alto, CA).

### Constructs

The different WDs were amplified by PCR using the following primers:

WD1, 5'-ATGCATCCATGGATTCCCGTCCGCCAGAAAAATAT-3' and 5'-GAAGATCTTCAATCCCACACCTTAATTGTAGCATC-3';  
WD2, 5'-ATGCATCCATGGTATGAGACTGGAGATTTGAACGA-3' and

5'-GAAGATCTTCAATCCCACATAGTTTAAATGGTCATA TC-3';  
WD3, 5'-ATGCATCCATGGTTTCAGGGCTTTGAATGCATCAGA-3' and 5'-GAAGATCTTCAATCCCACATT TTTATAGTTTTATC-3';  
WD4, 5'-ATGCATCCATGGGTGCAAACTGGCTACTGTGTGAAG-3' and 5'-GAAGATCTT CAGACCCATACACGCACAGTCTGGTC-3';  
WD5, 5'-ATGCATCCATGGGTAGCAACAAGGAATGCAAGGCT-3' and 5'-GAAGATCTTCAATCCCACATCTTAATAGTCTTGTC-3';  
WD6, 5'-ATGCATCCATGGGTGTCAGTACTGGCATGTGCCTTATG-3' and 5'-GAAGATCTTCAATCCCACATACGCGTAGGGTCTTGTC-3';  
WD7, 5'-ATGCATCCATGGTACAAGAACAAGCGATGCATGAAG-3' and 5'-GAAGATCTTCAACGGCACTCCCACACTTTTACTGT-3'.

All fragments were then ligated into the expression vector pRSET (Invitrogen, Leek, The Netherlands). FLAG-tagged and GST-tagged DCX constructs were described previously (12,15).

### Antibodies

Mouse polyclonal anti-doublecortin antibodies were produced against GST–DCX (12) using conventional protocols (32). Rabbit polyclonal anti-LIS1 antibodies (R19) were affinity purified (11). Anti-FLAG M2 monoclonal antibodies were purchased from Sigma. All secondary antibodies were from Jackson Immunoresearch (West Grove, PA); peroxidase-conjugated affinipure goat anti-mouse IgG (H+L), lissamine rhodamine-conjugated affinipure goat anti-mouse or anti-rabbit IgG (H+L), FITC-conjugated affinipure goat anti-mouse or anti-rabbit IgG (H+L).

### Immunostaining

Briefly, transfected COS-7 cells were plated on glass coverslips. After 48 h they were washed twice with phosphate-buffered saline (PBS), then fixed and permeabilized simultaneously as described (11). Primary neurons derived from embryonic rat hippocampus were obtained from Dr Tony Futerman. The neurons were fixed for 20 min with 4% PFA, 4% sucrose at

37°C and permeabilized for 5 min with 0.25% Triton X-100. After fixation the cells were incubated with 30 ml of the first antibody for 60 min at room temperature, then washed three times in PBS and incubated for 60 min with 30 ml of fluorescent-conjugated secondary antibodies. The coverslips were washed three times in PBS, drained and mounted. The immunostaining was visualized using an Olympus microscope (IX50 model; Hamburg, Germany) using the appropriate filters. Photography was with Kodak 160T film. Neurons were observed under a Bio-Rad (Hercules, CA) confocal microscope.

#### GST pull-down assay

GST fusion proteins were used for pull-down experiments with either recombinant LIS1 protein or brain extract. Recombinant 6×His-LIS1 was expressed in insect cells by *Baculovirus* [described by Sapir *et al.* (11)] and purified on Ni-NTA beads (Qiagen, Hilden, Germany). LIS1 and the different WD peptides were produced in the Rabbit Reticulocyte TnT System (Promega, Madison, WI) with [<sup>35</sup>S]methionine. In each pull-down experiment, 10 ml of the labeled reaction was used. E17 brain extract was prepared in T-T buffer (20 mM Tris-HCl pH 8, 100 mM NaCl, 1 mM EDTA, 0.1% Triton-X), supplemented with protease inhibitors (Sigma).

Recombinant proteins or brain extract were incubated with 10 mg of GST-DCX, GST-pep1, GST-pep2, GST-pep(1+2) and GST as control at 4°C for 15 h. Glutathione beads (20 ml) in 300 ml of T-T buffer were added to the protein mixture and rotated for 30 min at room temperature. After four washes with T-T buffer, 2× sample buffer was added and the beads were boiled and subjected to SDS-PAGE gel analysis. A western blot was performed with anti-LIS1 antibodies (monoclonal clone 210).

#### 6×His pull-down assay

Fifteen milligrams of 6×His-LIS1 were incubated with embryonic brain extract (prepared as described) at 4°C for 15 h. Ni-NTA beads (20 mg; Qiagen) in 400 ml of sonication buffer (300 mM NaCl, 50 mM sodium phosphate buffer pH 8.0) with 10 mM imidazole were added to the protein mixture and rotated at 4°C for 3 h. The beads were washed four times with sonication buffer with 30 mM imidazole and eluted with 20 µl of sonication buffer and 200 mM imidazole. After elution 5× sample buffer was added and the beads were run on an SDS-PAGE gel. A western blot was performed with mouse polyclonal anti-DCX antibodies.

#### Immunoprecipitation assay

Immunoprecipitation was performed in 293T cells using M2 beads (Sigma), or from E17 brain extract (prepared as described) using anti-LIS1 (monoclonal clone 338) and anti-GAD (monoclonal control) antibodies. Cell extract was prepared in IP buffer (50 mM Tris-HCl pH 7.5, 150 mM NaCl, 1% Triton X-100), supplemented with protease inhibitors (Sigma). Each 10 cm plate was washed with PBS, put on ice and scraped with 1 ml of cold IP buffer. The cells were incubated on ice for 15 min and were vortexed for 10 s every 5 min. After centrifugation at 9000 r.p.m. for 15 min at 4°C, 0.5 ml of the supernatant was rotated with M2 beads for 3 h at 4°C. Brain extract (~500 mg) was incubated with 5 ml of antibody for 15 h

at 4°C and then rotated with 20 ml A/G protein beads for 2 h at 4°C. Beads were washed four times with T-T or IP buffer, respectively. Sample buffer (×2) was added and the beads were boiled and subjected to an SDS-PAGE gel. A western blot was performed with anti-LIS1 (monoclonal clone 210) or anti-DCX antibodies.

#### Rate measurements

Tubulin was purified as described (11). The rate of tubulin assembly into polymers was monitored using a light scattering assay (12,15). Purified tubulin was diluted in PEM buffer (100 mM PIPES pH 6.9, 1 mM MgSO<sub>4</sub>, 1 mM EGTA) supplemented with 1 mM GTP, to a final concentration of 15 µM. GST-DCX, GST-LIS1 and GST (7.5 µg) were added to the purified tubulin subunits prior to measurement. Absorbance was measured at 350 nm at 1 min intervals in a Uvicon spectrophotometer (Kontron Instruments, Vineland, NJ) equipped with temperature controlled cells. Switching the temperature to 37°C induced assembly.

#### Competition assay

Sedimentation experiments were performed essentially as described (13). After microtubules (5 µM) were pre-assembled for 15 min at 37°C, GST-LIS1 and GST-DCX proteins were added. In each experiment one protein was at a constant concentration (2.5 µM) and the other at increasing concentrations (0–5 µM). All reactions were divided into three: 60% for Coomassie staining and 10% for western blot analysis with anti-DCX and anti-LIS1 antibodies, respectively.

#### ACKNOWLEDGEMENTS

The authors thank Dr Tony Futerman for the neurons. This work was supported in part by the Minerva Foundation, BSF grant no. 97-00014 and HFSP grant no. RG283199. O.R. is an Incumbent of Aser Rothstein Career Development Chair in Genetic Diseases.

#### REFERENCES

- Barkovich, A.J., Kuzniecky, R.I., Dobyns, W.B., Jackson, G.D., Becker, L.E. and Evrard, P. (1996) A classification scheme for malformations of cortical development. *Neuropediatrics*, **27**, 59–63.
- Reiner, O., Carrozzo, R., Shen, Y., Whernt, M., Faustinella, F., Dobyns, W.B., Caskey, C.T. and Ledbetter, D.H. (1993) Isolation of a Miller-Dieker lissencephaly gene containing G protein-β-subunit-like repeats. *Nature*, **364**, 717–721.
- des Portes, V., Pinard, J.M., Billuart, P., Vinet, M.C., Koulakoff, A., Carrie, A., Gelot, A., Dupuis, E., Motte, J., Berwald-Netter, Y. *et al.* (1998) A novel CNS gene required for neuronal migration and involved in X-linked subcortical laminar heterotopia and lissencephaly syndrome. *Cell*, **92**, 51–61.
- Gleeson, J.G., Allen, K.M., Fox, J.W., Lamperti, E.D., Berkovic, S., Scheffer, I., Cooper, E.C., Dobyns, W.B., Minnerath, S.R., Ross, M.E. *et al.* (1998) Doublecortin, a brain-specific gene mutated in human X-linked lissencephaly and double cortex syndrome, encodes a putative signaling protein. *Cell*, **92**, 63–72.
- Pilz, D.T., Matsumoto, N., Minnerath, S., Mills, P., Gleeson, J.G., Allen, K.M., Walsh, C.A., Barkovich, A.J., Dobyns, W.B., Ledbetter, D.H. *et al.* (1998) LIS1 and XLIS (DCX) mutations cause most classical lissencephaly, but different patterns of malformation. *Hum. Mol. Genet.*, **7**, 2029–2037.
- Harding, B. (1996) Gray matter heterotopia. In Guerrini, R. (ed.), *Dysplasias of Cerebral Cortex and Epilepsy*. Lippincott-Raven, Philadelphia, PA, pp. 81–88.

7. Neer, E., Schmidt, C.J. and Smith, T. (1993) LIS is more. *Nature Genet.*, **5**, 3–4.
8. Reiner, O., Cahana, A., Shmueli, O., Leeor, A. and Sapir, T. (1996) LIS1, a gene involved in a neuronal migration disorder: from gene isolation towards analysis of gene function. *Cell Pharmacol.*, **3**, 323–329.
9. Neer, E.J., Schmidt, C.J., Nambudripad, R. and Smith, T.F. (1994) The ancient regulatory-protein family of WD-repeat proteins. *Nature*, **371**, 297–300.
10. Hattori, M., Adachi, H., Tsujimoto, M., Arai, N. and Inoue, K. (1994) Miller-Dieker lissencephaly gene encodes a subunit of brain platelet-activating factor. *Nature*, **370**, 216–218.
11. Sapir, T., Elbaum, M. and Reiner, O. (1997) Reduction of microtubule catastrophe events by LIS1, platelet-activating factor acetylhydrolase subunit. *EMBO J.*, **16**, 6977–6984.
12. Horesh, D., Sapir, T., Francis, F., Caspi, M., Grayer Wolf, S., Elbaum, M., Chelly, J. and Reiner, O. (1999) Doublecortin, a stabilizer of microtubules. *Hum. Mol. Genet.*, **8**, 1599–1610.
13. Francis, F., Koulakoff, A., Boucher, D., Chafey, P., Schaar, B., Vinet, M.C., Friocourt, G., McDonnell, N., Reiner, O., Kahn, A. *et al.* (1999) Doublecortin is a developmentally regulated, microtubule-associated protein expressed in migrating and differentiating neurons. *Neuron*, **23**, 247–256.
14. Gleeson, J.G., Lin, P.T., Flanagan, L.A. and Walsh, C.A. (1999) Doublecortin is a microtubule-associated protein and is expressed widely by migrating neurons. *Neuron*, **23**, 257–271.
15. Sapir, T., Horesh, D., Caspi, M., Atlas, R., Burgess, H.A., Grayer Wolf, S., Francis, F., Chelly, J., Elbaum, M., Pietrokovski, S. *et al.* (2000) Doublecortin mutations cluster in evolutionary conserved functional domains. *Hum. Mol. Genet.*, **5**, 703–712.
16. Reiner, O., Albrecht, U., Gordon, M., Chianese, K.A., Wong, C., Sapir, T., Siracusa, L.D., Buchberg, A.M., Caskey, C.T. and Eichele, G. (1995) Lissencephaly gene (LIS1) expression in the CNS suggests a role in neuronal migration. *J. Neurosci.*, **15**, 3730–3738.
17. Fagerstam, L.G., Frostell-Karlsson, A., Karlsson, R., Persson, B. and Ronnberg, I. (1992) Biospecific interaction analysis using surface plasmon resonance detection applied to kinetic, binding site and concentration analysis. *J. Chromatogr.*, **597**, 397–410.
18. Jonsson, U. and Malmqvist, M. (1992) Real time biospecific interaction analysis: the integration of surface plasmon resonance detection, general biospecific interface chemistry, and microfluidics into one analytical system. In Turner, A. (ed.), *Advances in Biosensors*. JAI Press, London, UK, pp. 291–336.
19. Malmqvist, M. (1993) Biospecific interaction analysis using biosensor technology. *Nature*, **361**, 186–187.
20. Raghvan, M. and Bjorkman, P.J. (1995) BIAcore: a microchip-based system for analyzing the formation of macromolecular complexes. *Structure*, **15**, 331–333.
21. Sapir, T., Eisenstein, M., Burgess, H.A., Horesh, D., Cahana, A., Aoki, J., Hattori, M., Arai, H., Inoue, K. and Reiner, O. (1999) Analysis of lissencephaly-causing LIS1 mutations. *Eur. J. Biochem.*, **266**, 1011–1020.
22. Garcia-Higuera, I., Fenoglio, J., Li, Y., Lewis, C., Panchenko, M.P., Reiner, O., Smith, T.F. and Neer, E.J. (1996) Folding of proteins with WD-repeats: comparison of six members of the WD-repeat superfamily to the G protein  $\beta$  subunit. *Biochemistry*, **35**, 13985–13994.
23. Qian, F., Germino, F.J., Cai, Y., Zhang, X., Somlo, S. and Germino, G.G. (1997) PKD1 interacts with PKD2 through a probable coiled-coil domain. *Nature Genet.*, **16**, 179–183.
24. Tsiokas, L., Kim, E., Arnould, T., Sukhatme, V.P. and Walz, G. (1997) Homo- and heterodimeric interactions between the gene products of PKD1 and PKD2. *Proc. Natl Acad. Sci. USA*, **94**, 6965–6970.
25. Plank, T.L., Yeung, R.S. and Henske, E.P. (1998) Hamartin, the product of the tuberous sclerosis 1 (TSC1) gene, interacts with tuberin and appears to be localized to cytoplasmic vesicles. *Cancer Res.*, **58**, 4766–4770.
26. van Slegtenhorst, M., Nellist, M., Nagelkerken, B., Cheadle, J., Snell, R., van den Ouweland, A., Reuser, A., Sampson, J., Halley, D. and van der Sluijs, P. (1998) Interaction between hamartin and tuberin, the TSC1 and TSC2 gene products. *Hum. Mol. Genet.*, **7**, 1053–1057.
27. Nellist, M., van Slegtenhorst, M.A., Goedbloed, M., van den Ouweland, A.M., Halley, D.J. and van der Sluijs, P. (1999) Characterization of the cytosolic tuberin-hamartin complex. Tuberin is a cytosolic chaperone for hamartin. *J. Biol. Chem.*, **274**, 35647–35652.
28. Mattson, M.P. (1999) Establishment and plasticity of neuronal polarity. *J. Neurosci. Res.*, **57**, 577–589.
29. Fleck, M.W., Hirotsune, S., Gambello, M.J., Phillips-Tansey, E., Soares, G., Mervis, R.F., Wynshaw-Boris, A. and McBain, C.J. (2000) Hippocampal abnormalities and enhanced excitability in a murine model of human lissencephaly. *J. Neurosci.*, **20**, 2439–2450.
30. Qin, J., Mizuguchi, M., Itoh, M. and Takashima, S. (2000) Immunohistochemical expression of doublecortin in the human cerebrum: comparison of normal development and neuronal migration disorders. *Brain Res.*, **863**, 225–232.
31. Ausubel, F.M., Brent, R., Kingston, R.E., Moore, D.D., Seidman, J.G., Smith, J.A. and Struhl, K. (1992) *Current Protocols in Molecular Biology*, Vol. 1. Greene Publishing Associates and Wiley-Interscience, New York, NY.
32. Harlow, E. and Lane, D. (1988) *Antibodies: A Laboratory Manual*, Vol. 1. Cold Spring Harbor Laboratory Press, Cold Spring Harbor, NY.